The first osmium(II), ruthenium(II) and iron(II) complexes of [3$_n$]cyclophanes ($n = 2$–4): synthesis and electrochemical study[☆]

Teizi Satou [a,b], Ko Takehara [c], Mihoko Hirakida [a,b], Youichi Sakamoto [a,b], Hiroyuki Takemura [c], Hirokazu Miura [b,1], Mie Tomonou [b], Teruo Shinmyozu [a,*]

[a] *Institute for Fundamental Research of Organic Chemistry (IFOC), Kyushu University, Hakozaki 6-10-1, Higashi-ku, Fukuoka 812-8581, Japan*
[b] *Graduate School of Science, Kyushu University, Hakozaki 6-10-1, Higashi-ku, Fukuoka 812-8581, Japan*
[c] *Graduate School of Science, Kyushu University, Ropponmatsu 4-2-1, Chuo-ku, Fukuoka 810-8560, Japan*

Received 1 September 1998; received in revised form 9 October 1998

Abstract

(η^6-C$_6$H$_6$)(η^6-[3$_n$]Cyclophane)Ru(II) [BF$_4$]$_2$ and corresponding Os(II) [PF$_6$]$_2$, as well as bis(η^5-C$_5$H$_5$)(η^6,η^6-[3$_n$]cyclophane)Fe(II)Fe(II) [PF$_6$]$_2$ ([3$_n$]cyclophane = [3$_2$](1,4)cyclophane **2**, [3$_3$](1,3,5)cyclophane **3**, [3$_4$](1,2,3,5)cyclophane **4**, [3$_4$](1,2,4,5)cyclophane **5**) have been synthesized and characterized. The complexation shifts of the ^{1}H-NMR signals of the metal-bound aromatic protons (H$_b$) are ca. 0.5–0.7 and 0.1–0.4 ppm for Fe(II) and Ru(II) complexes, respectively, whereas those of Os(II) complexes are ca. $-$0.2–0.1 ppm. The complexation shifts of the ^{13}C-NMR signals of the tertiary aromatic carbons of the metal-bound benzene ring are ca. 39–42 and 45–50 ppm for Ru(II) and Os(II) complexes, respectively. Thus the ^{1}H- and ^{13}C-NMR chemical shifts of the metal-bound aromatic hydrogens and carbons are strongly influenced by the anisotropy effect of the metal. The Ru(II) complexes showed electrochemically reversible responses. In the case of Os(II) complexes, a well-defined cathodic peak was also observed, but the rising portion of the corresponding anodic peak was somewhat deviated from the ordinary CV profile. In both cases, the redox process was attributed to the two-electron one-step mechanism, M(II) $\rightleftharpoons$ M(0) (M = Ru and Os). An analysis of the redox properties of the Ru(II) and Os(II) complexes suggested that the Os(II)[3$_4$](1,2,4,5)cyclophane complex would be the most suitable subunit of an anticipated one-dimensional organometallic polymer. © 1999 Elsevier Science S.A. All rights reserved.

Keywords: Osmium; Ruthenium; Iron; Cyclophanes; π-Arene complexes; Cyclic voltammetry

1. Introduction

[m.n]Cyclophane (cyclophane = CP) with two short –(CH$_2$)$_m$– and –(CH$_2$)$_n$– bridges ($m = 2$, 3; $n = 2$, 3) has strong π-electron donating ability due to the transannular π–π interaction of the facing aromatic rings. Thus the cyclophane can serve as either a monodentate or bidentate π-ligand for transition metals [1] and lanthanides [2]. In [m.n]CP, the [3.3]system has stronger π-electron donating ability than the [2.2] and [2.3]systems, as was demonstrated by the charge transfer (CT) interaction of intra- [3] and intermolecular CT complexes of [m.n]CP [4]. The [3.3]system also has an advantage that it is less strained than the corresponding [2.2]- and [2.3]systems [5]. Our recent study revealed that [3$_n$]CP ($n = 2$–6) exhibits much stronger CT interaction than the corresponding [2$_n$]homolog ($n = 2$–6) [6] mainly because of the effective hyperconjugation between the benzyl hydrogens and the benzene rings due to the conformation favorable for π–σ interaction in the former [7]. The bending of the benzylic methylene groups out of the plane of the attached benzene ring

---

was expected to be 3.4° for [3_6]CP **1** [8] but 20° (20° by the X-ray structural analysis [6b]) for the corresponding [2_6]homolog by the semiempirical AM1 calculations [9]. Therefore the [3_n]CP is expected to be more suitable ligand than the corresponding [2_n]homolog. A large number of the complexes of Fe(II)- and Ru(II)-[2_n]CP have been synthesized so far [2], but few reports on the π-arene metal complexes of [3_n]CP have been appeared because of the much easier availability of [2_n]CP, especially of [2_2](1,4)CP which is commercially available, than the corresponding [3_n]homolog. Now [3_n]CP becomes much more readily available by the progress made in their synthesis [7,10].

In the pioneering work of the π-arene metal complexes of cyclophane, Boekelheide et al. extensively studied the synthesis, structure, and electrochemical properties of various mono- and dinuclear Ru(II) complexes of [2_n]CP ($n = 2$–6) as subunits of electrically conducting polymer [11]. As an important step toward this goal, they synthesized and characterized the mixed-valence ion of bis(η^6-C_6Me_6)[η^4,η^6-[2_4](1,2,4,5)CP]Ru(0)Ru(II) [BF_4]$_2$ (C_6-Me_6 = hexamethylbenzene) [11g]. The Fe(II)-[2_2](1,3)- and [2_2](1,4)CP complexes were prepared by Boekelheide et al. [12], Koray [13] and Rosenblum et al. [14]. In contrast to Ru–CP complexes, a limited number of Os complexes have been known; Tocher et al. synthesized and studied the structure of mononuclear Os(II) complexes, [Os(η^6-C_6H_6)(η^6-[2_2](1,4)CP][BF_4]$_2$, and trinuclear complexes, [(η^6-C_6H_6)Os(η^6,η^6-[2_2](1,4)CP)Ru(η^6,η^6-[2_2](1,4)CP)Os(C_6H_6)][BF_4]$_6$ [15]. Bandy et al. reported the synthesis and structure of Os(0) complexes, represented by [Os(η^6-C_6H_6)(η^4-C_6H_6)] [16]. However, no electrochemical study of the Os–cyclophane complexes has been reported so far.

Here we describe the first synthesis of the Ru(II), Os(II) and Fe(II) complexes of [3_n]CP ([3_n]CP = [3_2](1,4)CP **2**, [3_3](1,3,5)CP **3**, [3_4](1,2,3,5)CP **4**, [3_4](1,2,4,5)CP **5**), and electrochemical properties of Ru(II) and Os(II) complexes. A final goal of this fundamental study is directed toward the development of new electrically conducting and magnetic materials first proposed by Boekelheide [1, 11b].
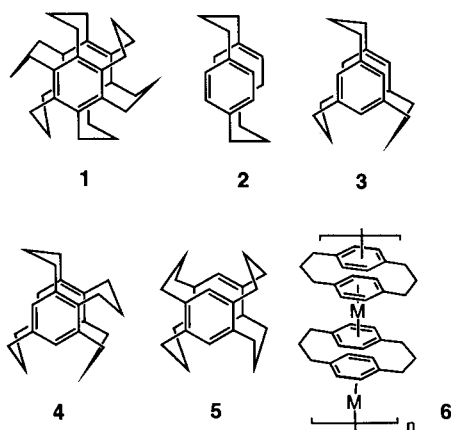

2. Results and discussion

2.1. Synthesis

Gill and Mann developed a general synthetic method of cyclopentadienyl (cp) capped (η^6-arene)Fe(II) complexes by the visible-light irradiation of (η^5-cp)(η^6-p-xylene)Fe(II) cations in the presence of suitable ligands [17a], and they demonstrated that this method was applicable to the synthesis of the (η^5-cp)(η^6-[2_2](1,4)CP)Fe(II) complex [17b]. Alternatively, the $AlCl_3$ catalyzed ligand exchange between arenes and ferrocene, first described by Nesmeynov et al. [18] and later elaborated by Sutherland et al. [19], has been used to prepare a wide range of complexes of the type [(η^5-cp)(η^6-arene)Fe(II)]X$^-$, where X is PF_6 or BF_4. The use of [2_n]CP as a ligand in the photolysis allowed the preparation of mono-cp capped complexes such as [2_2](1,3) [12a] and [2_2](1,4)CP complexes [12b], whereas di-cp capped complexes of [2_2](1,3) [12a] and [2_2](1.4)CP [12b, 13] were predominantly formed when more than 2 M equivalents of ferrocene were used in the ligand exchange. Relatively unstable bis(η^6-[2_2](1,4)CP)Fe(I) complexes were synthesized in a similar way [14]. An application of this ligand exchange to [3_n]CP **2**–**4** afforded bis(η^5-cp)(η^6,η^6-[3_n]CP)Fe(II)-Fe(II) [PF_6] **8**–**10** as tan crystals in good yields (Scheme 1).

Bennett et al. developed a general synthetic method of (η^6-arene^1)(η^6-arene^2)Ru(II) complexes by treatment of [RuCl$_2$(η^6-arene^1)]$_2$ with acetone and $AgBF_4$, followed by CF_3COOH and arene^2 [20]. Applying the method to [2_n]CP ligands, Boekelheide et al. prepared various Ru(II) complexes of [2_n]CP of the type (η^6-C_6Me_6)(η^6-[2_n]CP)Ru(II) [11a,b,d,e,f] and bis(η^6-C_6Me_6)(η^6,η^6-[2_n]CP)Ru(II)Ru(II) [11c,g,h,i,j]. The corresponding [3_n]CP complexes of the former type, [(η^6-C_6H_6)(η^6-[3_n]CP)Ru(II)] [BF_4^-]$_2$ **13**–**16**, were prepared by the reaction of [(η^6-C_6H_6)Ru(II)(acetone)$_3$], which was derived from [(η^6-C_6H_6)RuCl$_2$]$_2$ **12** and acetone, and the corresponding [3_n]CP (Scheme 2). The bis(η^6-[3_2](1,4)CP)Ru(II) complex **19** was also prepared in a similar way via dinuclear Ru(II) complex **18** (Scheme 3).

In principle, the (η^6-C_6H_6)(η^6-arene)Os(II) complexes can be prepared by the reaction of [(η^6-C_6H_6)Os(II)(acetone)$_3$]$^{2+}$ with arenes in CF_3COOH as was reported by Mann et al. [21]. Tocher et al. synthesized [(η^6-C_6H_6)(η^6-[2_2](1,4)CP)Os(II)][BF_4]$_2$ from [(η^6-C_6H_6)OsCl$_2$]$_2$ via the acetone solvate [15] according to the Bennet procedure [20]. They also prepared trinuclear heterometallic complex [(η^6-C_6H_6)Os(η^6,η^6-[2_2](l,4)CP)Ru(η^6,η^6-[2_2](1,4)-CP)Os(η^6-C_6H_6)] [BF_4]$_6$ by a similar procedure [15a]). The Os(II) complexes of [3_n]CP **21**–**24** were prepared as PF_6^- salts according to the Mann procedure [21] by the reaction of (η^6-
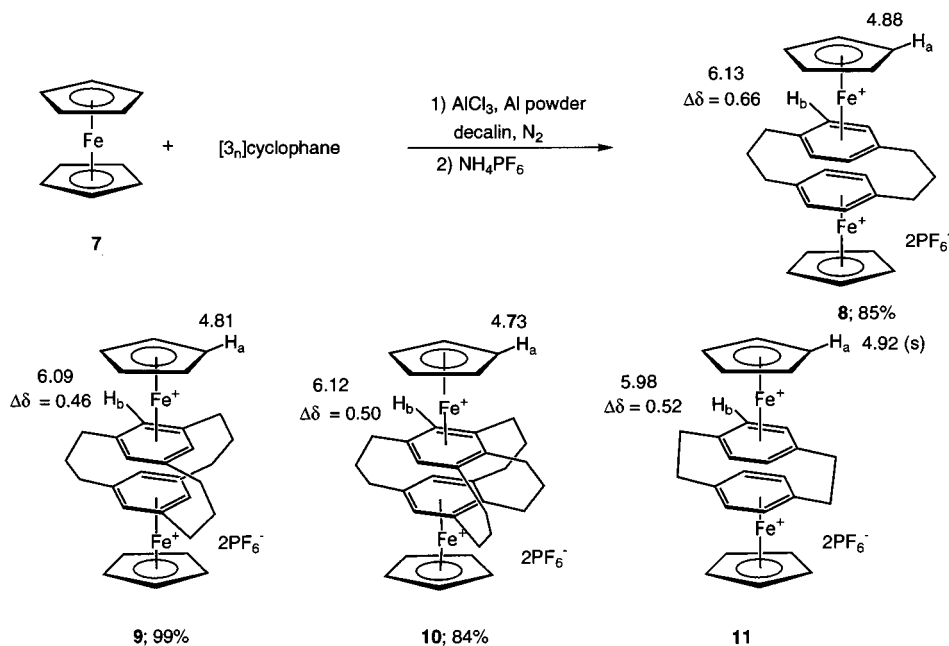
Scheme 1. Synthesis of Fe(II) complexes of [3$_n$]cyclophanes **8**–**10** and their ¹H-NMR data of the aromatic protons (270 MHz, [D$_6$]acetone). The ¹H-NMR data of **11** are also shown as a reference. The $\Delta\delta$ shows the complexation shift [$\Delta\delta = \delta$ (free ligand in [D$_6$]acetone) $- \delta$ (complex in [D$_6$]acetone).

C$_6$H$_6$)Os(CH$_3$CN)$_3$Cl$_2$ **20**, which was derived from (NH$_4$)$_2$OsCl$_6$ [22], with acetone followed by the corresponding [3$_n$]CP (Scheme 4). All Fe(II), Ru(II) and Os(II) complexes thus prepared were air-stable in the solid state, but the Fe(II) complexes underwent slow decomposition on exposure to air in solution.

2.2. Spectral properties

The chemical shifts of the aromatic proton signals of the Fe(II) complexes **8**–**10** in [D$_6$]acetone, Ru(II) complexes **13**–**16** and **19** in CD$_3$CN and Os(II) complexes **21**–**24** in CD$_3$CN are shown in Schemes 1–4, respectively. The $\Delta\delta$ denotes the complexation shift [23]: $\Delta\delta = \delta$ (free cyclophane) $- \delta$ (complex) where the δ values of a free cyclophane and its complex are measured in the same solvent. The $\Delta\delta$ was 0.46–0.66 ppm (**8**, 0.66; **9**, 0.46; **10**, 0.50 ppm) for the Fe(II)-bound aromatic protons H$_b$ of the di-cp capped Fe(II) complexes **8**–**10**, and the largest $\Delta\delta$ value (0.66) was observed in the complex with the least bridge **8**, and the value was comparable to that of the corresponding [2.2]homolog **11**. Similar higher field shifts of the metal-bound aromatic protons H$_b$ were observed in the ¹H-NMR spectra of the Ru(II) complexes (**13**, $\Delta\delta = 0.36$; **14**, 0.08; **15**, 0.15; **16**, 0.32 ppm), but no correlation between the magnitude and the number of the bridges was observed. The compound **17** showed larger $\Delta\delta$ values for both H$_b$ and H$_c$ protons than its higher homolog **13**. The dicyclophane capped complex **19** showed the largest $\Delta\delta$ value (0.71 ppm) and this was

attributed to an enhanced diamagnetic ring current of the facing cyclophanes. The aromatic proton signals H$_c$ of the Ru unbound deck shifted downfield but the magnitude was almost the same (**13**, $\Delta\delta = -0.31$; **14**, -0.36; **15**, -0.32; **16**, -0.20 ppm). Similarly the H$_a$ proton signals of **13**–**17** appeared at similar positions and no appreciable difference was observed.

In sharp contrast to the ¹H-NMR properties of the Ru(II) complexes, complexation of the Os(II) metal caused the metal-bound H$_b$ protons to shift slightly downfield except for **21** where the effect was almost zero (**21**, $\Delta\delta = 0.08$; **22**, -0.20; **23**, -0.13; **24**, -0.05 ppm). The Os(II)-unbound aromatic protons H$_c$ showed further down field shifts (**21**, $\Delta\delta = -0.39$; **22**, -0.41; **23**, -0.39; **24**, -0.30 ppm). A similar trend was also observed in the H$_a$ proton signals. Thus the shielding effect of the Ru(II) metal was more significant than that of the Os(II) metal [21a].

The ¹³C-NMR data of the Ru(II) and Os(II) complexes are shown in Scheme 5. Binding of the metal(II) ions to cyclophane greatly enhances upfield shifts of the metal-bound aromatic tertiary (C$_t$) and quaternary (C$_q$) carbon signals, whereas metal-unbound aromatic carbon signals shift to slightly down field as compared with the corresponding carbon signals of the free cyclophane ligand. The complexation shifts [$\Delta\delta = \delta$ (free cyclophane in CDCl$_3$) $- \delta$ (complex in CD$_3$CN) of the tertiary and quaternary aromatic carbons are ca. 39–42 and 16–24 ppm for the Ru(II) complexes, respectively, whereas they are ca. 45–50 and 21–28 ppm for the Os(II) complexes. The magnitude of the complexation
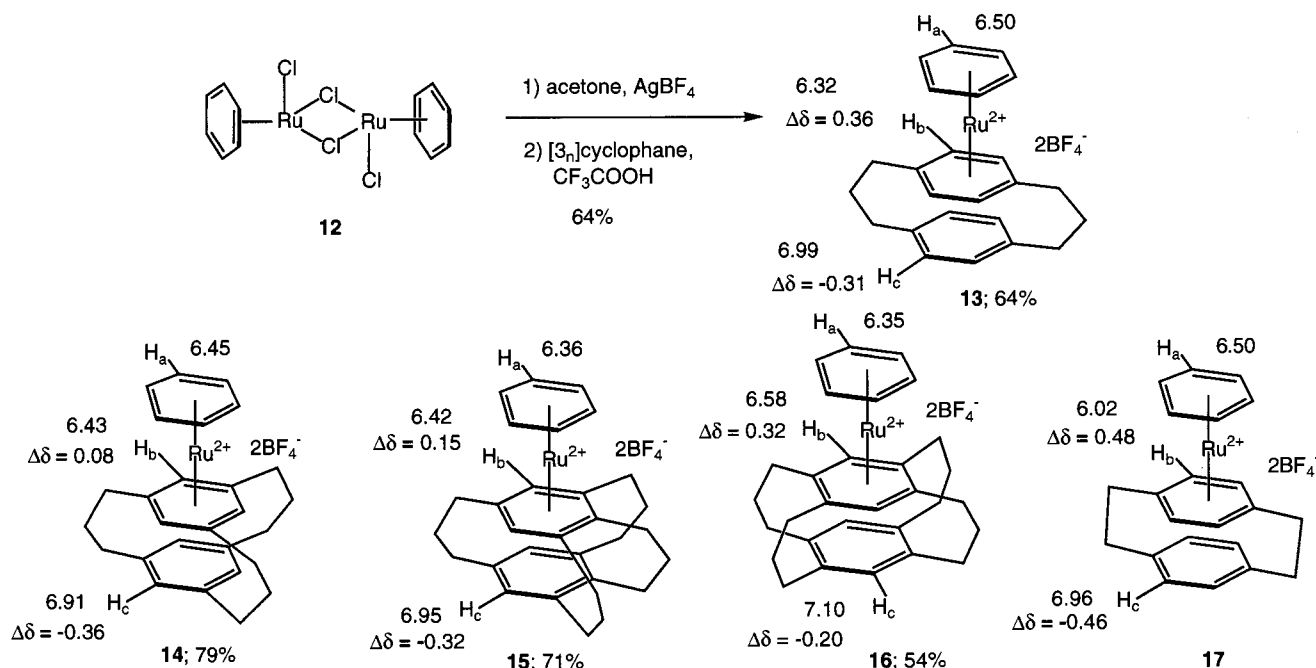
Scheme 2. Synthesis of Ru(II) complexes of [3$_n$]cyclophanes **13**–**16** and their ^{1}H-NMR data of the aromatic protons (270 MHz, CD$_3$CN). The ^{1}H-NMR data of **17** are also shown as a reference. The $\Delta\delta$ shows the complexation shift [$\Delta\delta = \delta$ (free ligand in CD$_3$CN) $- \delta$ (complex in CD$_3$CN).

shifts is almost independent on the number of the bridges but slightly dependent on the metal; the shift is more significant in the Os(II) complexes than in the corresponding Ru(II) complexes. Thus both ^{1}H- and ^{13}C-NMR data suggested that the chemical shifts of the aromatic protons and carbons of the complexes were influenced by the anisotropy effect of the metal.

For the determination of the molecular weight of the metal complexes, FAB MS in *m*-nitrobenzyl alcohol as a matrix proved to be very useful, and the M–[BF$_4^-$] peaks for the Ru(II) complexes as well as M–[PF$_6^-$] peaks for the Fe(II) and Os(II) complexes were clearly observed in each case. In the IR spectra (KBr) of the Ru(II) and Os(II) complexes, new bands with medium intensities appeared in the region of 3030–3100 cm^{-1} and these bands may be assigned to the C–H stretching frequencies of the metal-bound benzene rings.
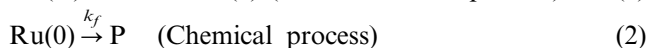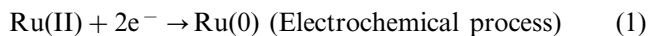
2.3. Electrochemical properties

Fig. 1 shows the cyclic voltammograms (CVs) of the Ru(II) complexes **13** ($n = 2$), **14** ($n = 3$), **15** ($n = 4$) and **16** ($n = 4$) in CH$_3$CN/0.1 M Bu$_4$NClO$_4$ solution at the potential scan rate of 0.1 V s^{-1}. The cathodic peak P_c appeared at -1.07, -1.16, -1.19, and -1.12 V (vs. Ag | AgNO$_3$) for **13**–**16**, respectively. The corresponding anodic peak P_a was very small at this potential scan rate, but the peak current of P_a, I_{pa}, gradually increased with increasing potential scan rate (Fig. 2) and the I_{pa}/I_{pc} ratio approached unity at higher scan rates for

the CVs of **13**–**15** (Fig. 3). Fig. 4 denotes the CVs at the potential scan rate of 6.4 V s^{-1}. The redox potentials $E_{1/2}$ obtained as the mid-point potential of the cathodic and anodic potentials were -1.04, -1.13, -1.15 and -1.08 V for **13**–**16**, respectively.

In the CVs of a series of (η^6-C$_6$Me$_6$)(η^6-[2$_n$]CP)Ru(II) complexes ([2$_n$]CP = [2$_6$](1,2,3,4,5,6)CP, [2$_4$](1,2,3,5)CP, [2$_4$](1,2,4,5)CP) [11d], Boekelheide et al. reported that the Ru(II) was reduced to Ru(0) with the two-electron one-step mechanism at potential range from -0.5 to -1.0 V (vs. Ag | AgNO$_3$) [11d,f,g]. Even in the case of a consecutive one-electron twostep reduction mechanism (Ru(II)→Ru(I) and Ru(I)→Ru(0)), the two reduction peaks were reported to appear in a close proximity [24] as in the case of the [(η^6-C$_6$Me$_6$)(η^6-[2$_4$](1,2,3,5)CP)Ru(II) complex [11d]. Therefore we attributed the cathodic peak P_c and the corresponding anodic peak P_a to the reduction of Ru(II) to Ru(0) and to the reoxidation of Ru(0) to Ru(II), respectively as shown in Scheme 6.

As discussed by Nicholson and Shain [25], the change in peak current ratio, I_{pa}/I_{pc}, is characteristic of the reversible electrochemical reaction followed by irreversible chemical reaction (E_rC_i mechanism) which produces an electrochemically inactive final product P.

$$Ru(II) + 2e^- \rightarrow Ru(0) \text{ (Electrochemical process)} \quad (1)$$

$$Ru(0) \overset{k_f}{\rightarrow} P \quad \text{(Chemical process)} \quad (2)$$

By adapting this mechanism to the present case, we expected that the Ru(0) species was not so stable and
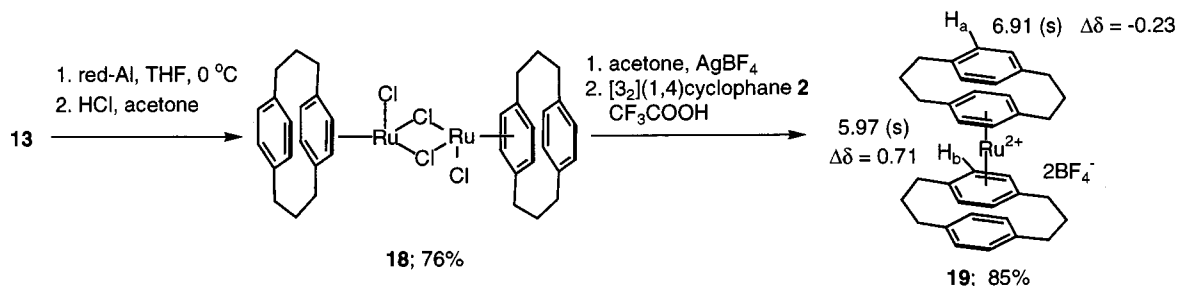
Scheme 3. Synthesis of Ru(II) complex **19** and its ^{1}H-NMR data of the aromatic protons (270 MHz, CD$_3$CN). The $\Delta\delta$ shows the complexation shift [$\Delta\delta = \delta$ (free ligand in CD$_3$CN) $- \delta$ (complex in CD$_3$CN)].

gradually converted into the electrochemically inactive form. Such a mechanism incorporating the chemical process was consistent with the reported mechanism for the similar Ru(II) complexes [11d,h]. Based on the analysis of Nicholson and Shain [25], we estimated the rate constants (k_f) of the chemical process in Eq. (2) to be 3.4, 1.2, 1.6 and 0.15 s^{-1} for **13**–**16**, respectively (Fig. 5) [26,27]. This result indicated that the decomposition rate of the Ru(0) to P was much faster at **13** than at **14** and **15**, and was much slower at **16** than at **14** and **15**. The CVs of the CH$_3$CN solutions of the Ru(II) free ligands **2**–**5** did not show any redox peak in the potential range from $+1.0$ to -2.0 V.

The Os(II) complexes **21** ($n = 2$), **22** ($n = 3$), **23** ($n = 4$) and **24** ($n = 4$) showed similar CV responses to the Ru(II) complexes in CH$_3$CN/0.1 M Bu$_4$NClO$_4$ solution at the potential scan rate of 0.1 V s^{-1}. The rising portion of the anodic peak was somewhat deviated from the ordinary CV profiles and the peak shifted to the anodic side (Fig. 6). Although this shift made it difficult to analyze quantitatively the redox potential $E_{1/2}$ and the decomposition rate constant k_f of the Os(II) complexes, the cathodic peak potential E_{pc} appeared at -1.15, -1.26, -1.32 and -1.13 V (vs. Ag | AgNO$_3$) for **21**–**24**, respectively. Fig. 7 denotes the CVs at the potential scan rate of 6.4 V s^{-1}. The I_{pa}/I_{pc} ratio of the Os(II) complexes was larger than that of the corresponding Ru(II) complexes at a given scan rate. This result indicated that the Os(0) state was more stable to the chemical decomposition than the corresponding Ru(0) state. The E_{pc} values suggested that [3$_2$](1,4)CP and [3$_4$](1,2,4,5)CP moieties in **13** and **16**, respectively, could take boat-shaped geometries required for η^4-bonding more easily than [3$_3$](1,3,5)CP and [3$_4$](1,2,4,5)CP moieties in **14** and **15**, respectively, since the benzene ring of [3$_2$](1,4)CP **2** has a boat-shaped geometry with the distortion angles being 6.4° [5b] as shown in Scheme 6, and [3$_4$](1,2,4,5)CP **5** has a preformed, near-optimum boat-shaped geometry to bind η^4 [28]. A similar phenomenon was reported in the CVs of the Ru(II) complexes of a series of [2$_n$]cyclophanes [11d]. The boat-type deformation is

favorable for the formation of the η^4-M(0) state from the η^6-M(II) state, and this geometrical change is reported to be the controlling factor affecting the reduction potential of Ru(II) to Ru(0) state [11d]. The two-electron one-step mechanism and the geometrical change accompanying the reduction of Ru(II) to Ru(0) were well established [29], and some Ru(0) complexes were isolated and characterized [11f, 29]. Smaller E_{pc} values of **16** and **24**, both of which contained [3$_4$](1,2,4,5)CP **5** as the ligand, and the slowest decomposition rate of Ru(0) state in **16**, as well as slower decomposition rate of the Os(0) state than the corresponding Ru(0) state suggested that the best metal-ligand combination was the Os(II) and [3$_4$](1,2,4,5)CP **5** for the subunit of anticipated metal polymer.

The E_{pc} value may be affected not only by the molecular geometry of the ligand but by electron donating ability of the ligand; the benzene ring with preformed boat-shaped geometry for η^4-bonding of M(0) state shifts the E_{pc} to more positive potentials, whereas the strong electron donating ligand may stabilizes the M(II) state more strongly than the M(0) state and, therefore, shifts the E_{pc} to more negative potentials. The E_{pc} values of parent (η^6-C$_6$H$_6$)(η^6-C$_6$H$_6$)Ru(II) [BF$_4$]$_2$ **25** (-1.02 V), **13** (-1.07 V) and **19** (-1.19 V vs. Ag/AgNO$_3$), shown in Fig. 8, suggested that the ΔE_{pc} (-0.12 V) between **19** and **13** was ascribed to the much enhanced π-electron donating ability of [3$_2$](1,4)CP than benzene itself, whereas the ΔE_{pc} (0.05 V) between **13** and **25** was ascribed to the combined effect of the enhanced π-electron donating ability of [3$_2$](1,4)CP in **13** and its preformed boat-shaped geometry for η^4-bonding (Scheme 6).

On the second redox peaks P_c' and P_a' observed in the CVs of **13** and **21**, the increase of the I_{pa}'/I_{pc}' ratio with decreasing scan rates (Fig. 2) was an indication of the participation of the product of the irreversible chemical process such as an $E_r C_i E_r$ mechanism. However, we have no clear explanation of the possible species in this process at the present stage. In the case of the Fe(II) complexes **8**–**10**, no clear redox peak was observed at the potential range between -1.0 and $+1.25$ V.
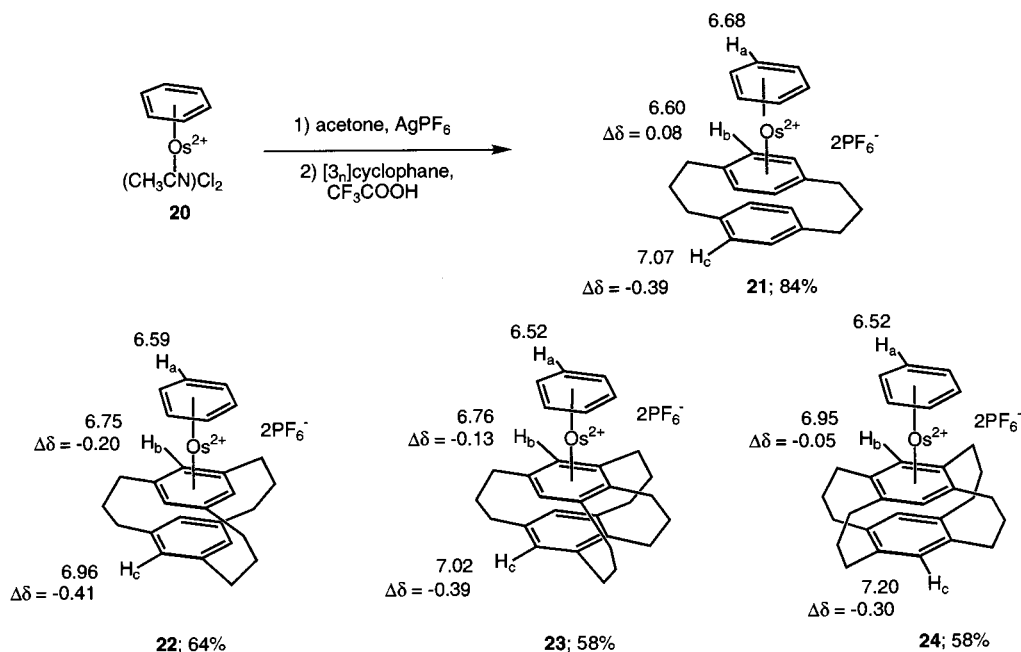
Scheme 4. Synthesis of Os(II) complexes of [3$_n$]cyclophanes **21**–**24** and their ^{1}H-NMR data of the aromatic protons (270 MHz, CD$_3$CN). The $\Delta\delta$ shows the complexation shift [$\Delta\delta = \delta$ (free ligand in CD$_3$CN) $- \delta$ (complex in CD$_3$CN)].

3. Summary

The first Fe(II), Ru(II) and Os(II) complexes of [3$_n$]CP were synthesized and characterized. Both of the ^{1}H and ^{13}C-NMR data of these complexes suggested that the chemical shifts of the aromatic protons and carbons of the complexes were more strongly influenced by the anisotropy effect of the metal than by the ring current effects of the aromatic rings. The shift of the E_{pc} value of the Ru(II) complex **13**–**16** to more negative potentials than that of the corresponding [2$_n$]homolog indicated the much stronger π-electron donating ability and less deformed benzene ring of the [3$_n$]CP than the corresponding [2$_n$]CP. An analysis of the redox properties of the Ru(II) and Os(II) complexes of [3$_n$]CP suggested that the Os(II)[3$_4$](1,2,4,5)CP complex would be the most suitable subunit of an anticipated one-dimensional organometallic polymer. The synthetic and electrochemical study of Ru(II)Ru(II) and Os(II)Os(II) complexes of [3$_4$](1,2,4,5)CP **5** is in progress and will be reported elsewhere.

4. Experimental details

4.1. General
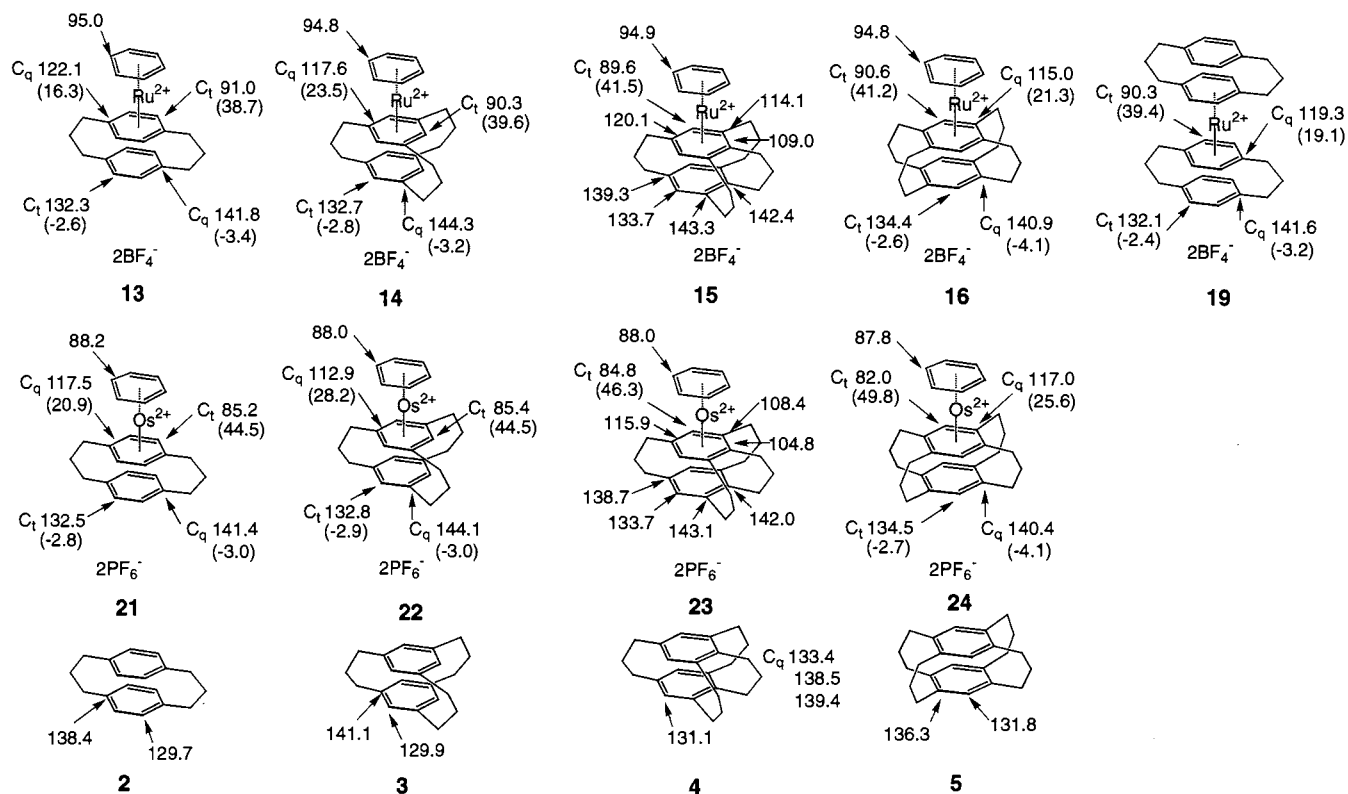
^{1}H-NMR spectra were recorded on JEOL JNM-EX 270 and 400, and measured in CDCl$_3$, CD$_3$CN, or DMSO-d_6 with Me$_4$Si as an internal standard. ^{13}C-NMR spectra were recorded on JEOL JNM-EX 270 and 400, and measured in CDCl$_3$ or CD$_3$CN with

Me$_4$Si as an internal standard. FAB MS were taken with a JEOL JMS-SX/SX 102A tandem mass spectrometer using *m*-nitrobenzyl alcohol as matrix. IR spectra were measured with HITACHI I-5040 FT-IR spectrometer. Elemental analyses were performed by the Service Centre of the Elementary Analysis of Organic Compounds affiliated with the Faculty of Science, Kyushu University.

The compounds [(η^6-C$_6$H$_6$)RuCl$_2$]$_2$ **11** and [(η^6-C$_6$H$_6$)Os(CH$_3$CN)Cl$_2$] **20** were prepared according to the Bennett [20] and the Mann [21] procedure, respectively. [2$_2$](1,4)CP was purchased from Tokyo Kasei Kogyo Co., Ltd. The Fe(II) and Ru(II) complexes **11** [12b] and **17** [11a] were prepared according to the literature procedures. [3$_2$](1,4)CP **2** [10d], [3$_3$](1,3,5)CP **3** [7b, 10c], [3$_4$](1,2,3,5)CP **4** [7b], [3$_4$](1,2,4,5)CP **5** [10e] were prepared by the reported procedures.

Cyclic voltammograms were recorded by a Fuso Model 311 polarographic analyzer, a Model 321B potential-sweep unit, and a Yokogawa Model 3655 digital recorder. A glassy carbon (GC) disk-electrode (Bioanalytical Systems Inc., 3 mm diameter), an Ag/0.01 M AgNO$_3$/0.1 M Bu$_4$NClO$_4$ (CH$_3$CN) electrode and a platinum wire were used as the working electrode, the reference electrode and the counter electrode, respectively. All potential values were reported versus the reference electrode. The measurements were done in deoxygenated CH$_3$CN solution containing 1 mM (1 M = 1 mol dm^{-3}) complex as the redox species and 0.1 M Bu$_4$NClO$_4$ as the supporting electrode. All the measurements were done at 25 ± 0.1°C.

13

95.0
C_q 122.1 (16.3)   Ru^{2+} C_t 91.0 (38.7)
C_t 132.3 (-2.6) C_q 141.8 (-3.4)
2BF$_4^-$

14

94.8
C_q 117.6 (23.5)   Ru^{2+} C_t 90.3 (39.6)
C_t 132.7 (-2.8) C_q 144.3 (-3.2)
2BF$_4^-$

15

94.9
C_t 89.6 (41.5)   Ru^{2+} 114.1
120.1   109.0
139.3   142.4
133.7   143.3
2BF$_4^-$

16

94.8
C_t 90.6 (41.2)   Ru^{2+} C_q 115.0 (21.3)
C_t 134.4 (-2.6) C_q 140.9 (-4.1)
2BF$_4^-$

19

94.8
C_t 90.3 (39.4)   Ru^{2+} C_q 119.3 (19.1)
C_t 132.1 (-2.4) C_q 141.6 (-3.2)
2BF$_4^-$

21

88.2
C_q 117.5 (20.9)   Os^{2+} C_t 85.2 (44.5)
C_t 132.5 (-2.8) C_q 141.4 (-3.0)
2PF$_6^-$

22

88.0
C_q 112.9 (28.2)   Os^{2+} C_t 85.4 (44.5)
C_t 132.8 (-2.9) C_q 144.1 (-3.0)
2PF$_6^-$

23

88.0
C_t 84.8 (46.3)   Os^{2+} 108.4
115.9   104.8
138.7   142.0
133.7   143.1
2PF$_6^-$

24

87.8
C_t 82.0 (49.8)   Os^{2+} C_q 117.0 (25.6)
C_t 134.5 (-2.7) C_q 140.4 (-4.1)
2PF$_6^-$

2
138.4   129.7

3
141.1   129.9

4
C_q 133.4   138.5   139.4   131.1

5
136.3   131.8

Scheme 5. ^{13}C-NMR data of aromatic carbons of the Ru(II) and Os(II) complexes **14–16**, **19**, **21–24** (68 or 100 MHz, CD$_3$CN) as well as the free cyclophanes **2–5** in CDCl$_3$. The $\Delta\delta$ shows the complexation shift [$\Delta\delta = \delta$(free ligand in CDCl$_3$) − δ (complex in CD$_3$CN).

4.2. Synthesis of Fe(II) complexes, 8–10

Bis(η^5 - cyclopentadienyl)(η^6,η^6 - [3$_2$](1,4)CP)diiron-(II,II) bis(hexafluorophosphate) **8**. A mixture of [3$_2$](1,4)cyclophane **2** (204 mg, 0.864 mmol), ferrocene (820 mg, 4.40 mmol), AlCl$_3$ (1.64 g, 12.3 mmol), A1 powder (31 mg, 1.15 mmol), and dry decalin (20 ml) was heated at 160°C for 2 h under an Ar atmosphere. The dark green reaction mixture was cooled in an ice bath before dropwise addition of distilled water (20 ml). The content of the flask was transferred to a separatory funnel with water (40 ml) and Et$_2$O (40 ml). The aqueous layer was separated, washed with Et$_2$O (2 × 20 ml), and filtered. To the filtrate was added a solution of NH$_4$PF$_6$ (1.8 g, 11.0 mmol) in water (3 ml). The precipitate was collected by filtration and dried in vacuo at

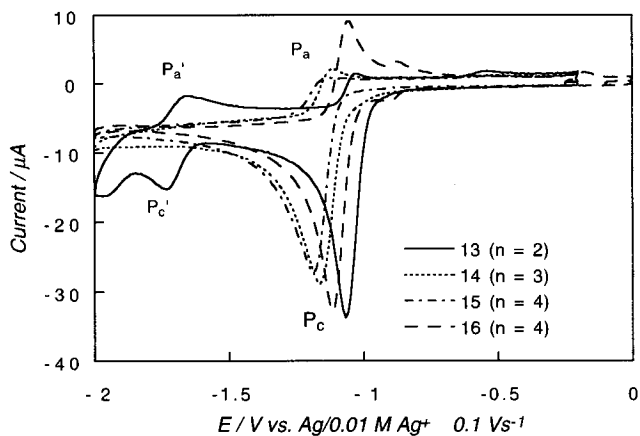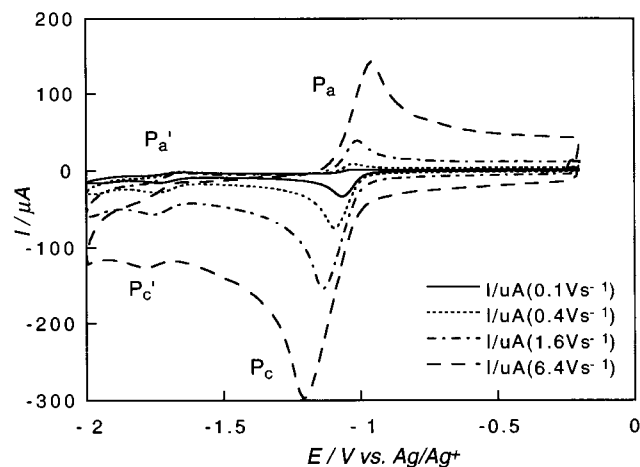Fig. 1. Cyclic voltammograms of 1 mM **13–16** in CH$_3$CN/0.1 M Bu$_4$NClO$_4$ observed at a GC electrode and potential scan rate is 0.1 V s^{-1}.

Fig. 2. Cyclic voltammograms of 1 mM **13** in CH$_3$CN/0.1 M Bu$_4$NClO$_4$ observed at a GC electrode and various potential scan rates (0.1–6.4 V s^{-1}). In this Figure, the cathodic peak currents at 0.1, 0.4 and 1.6 V s^{-1} were normalized to that of 6.4 V s^{-1}.
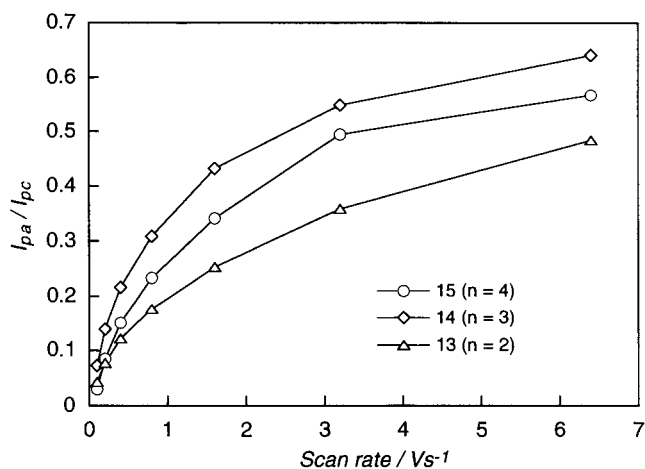
Fig. 3. Plots of the peak current ratio of P_a to P_c, $I_{pa}/I_{pc'}$ as a function of a potential scan rate for **13**–**15**.

room temperature (r.t.) to give **8** as tan powder (554 ma, 85%). ^{1}H-NMR (270 MHz, [D$_6$]acetone): $\delta = 2.31$ (m, 4H, –CH$_2$CH$_2$CH$_2$–); 2.91 (m, 8H, –CH$_2$CH$_2$CH$_2$–); 4.88 (s, 10H, Cp); 6.13 (s, 8H, ArH). FAB MS: m/z 623 [M$^+$ –PF$_6^-$]. Found: C, 45.08; H 4.16. Calc. for C$_{25}$H$_{30}$F$_{12}$Fe$_2$P$_2$·C$_6$H$_6$O (acetone): C, 45.06; H, 4.16.

Bis(η^5-cyclopentadienyl)(η^6,η^6-[3$_3$](1,3,5)cyclophane)-diiron(II,II) bis(hexafluorophosphate) **9**: Yield 601 mg (99%), tan crystals (acetone-pentane). ^{1}H-NMR (270 MHz, [D$_6$]acetone): $\delta = 2.2$–3.2 (m, 18H, –CH$_2$CH$_2$CH$_2$–); 4.81 (s, 10H, Cp); 6.09 (s, 6H, ArH). FAB MS: m/z 663 [M$^+$ –PF$_6^-$]. Found: C, 47.12; H, 4.71. Calc. for C$_{31}$H$_{34}$F$_{12}$Fe$_2$P$_2$·C$_6$H$_6$O (acetone) (866.3): C, 47.14; H, 4.65.

Bis(η^5-cyclopentadienyl)(η^6,η^6-[3$_4$](1,2,3,5)cyclo-phane)diiron(II,II) bis(hexafluorophosphate) **10**. Yield 227 mg (84%), tan crystals (acetone–pentane). ^{1}H-NMR (270 MHz, [D$_6$]acetone): $\delta = 2.3$–3.4 (m, 24H,
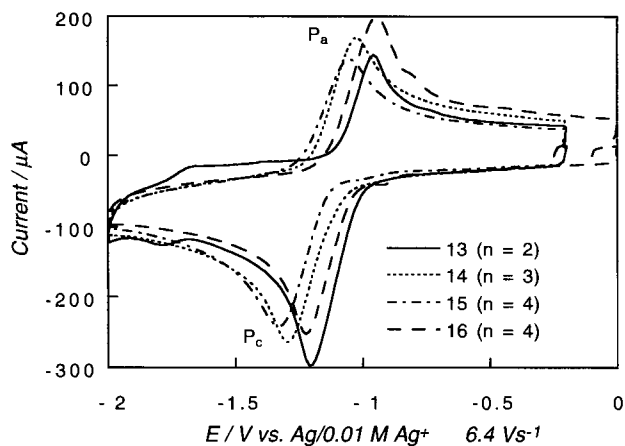

Fig. 4. Cyclic voltammograms of 1 mM **13**–**16** in CH$_3$CN/0.1 M Bu$_4$NClO$_4$ observed at a GC electrode and potential scan rate of 6.4 V s^{-1}.

–CH$_2$CH$_2$CH$_2$–); 4.73 (s, 10H, Cp); 6.12 (s, 4H, ArH). FAB MS: m/z: 703 [M$^+$ –PF$_6^-$]. Found: C, 49.05; H, 4.78. Calc. for C$_{34}$H$_{38}$F$_{12}$Fe$_2$P$_2$·C$_6$H$_6$O (acetone) (906.4): C, 49.03; H, 4.89.

4.3. Synthesis of Ru(II) complexes, 13–16

(η^6 - Benzene)[η^6 - [3$_2$](1,4)cyclophane]ruthenium(II) bis(tetrafluoroborate) **13**: [(η^6-Benzene)RuCl$_2$]$_2$ **12** (195 mg, 0.391 mmol), AgBF$_4$ (335 mg, 1.72 mmol), and acetone (8 ml) were stirred at r.t. for 35 min under N$_2$. The precipitated AgCl was removed by filtration and washed with acetone (ca. 4 ml). To the filtrate was added [3$_2$](1,4)cyclophane **2** (173 mg, 0.732 mmol) and CF$_3$COOH (10 ml), and the mixture was refluxed for 35 min under N$_2$. The cooled reaction mixture was diluted with Et$_2$O (50 ml), and the resulting precipitate was collected by filtration, washed with Et$_2$O, and dried in vacuo at r.t. overnight to afford **13** (275 mg, 64%), faintly greenish yellow crystals (CH$_3$CN–Et$_2$O). ^{1}H-NMR (400 MHz, CD$_3$CN): $\delta = 2.24$–2.83 (m, 12H, –CH$_2$CH$_2$CH$_2$–); 6.32 (s, 4H, H$_b$); 6.50 (s, 6H, H$_a$); 6.99 (s, 4H, H$_c$). ^{13}C-NMR (68 MHz, CD$_3$CN): $\delta =$ 141.8; 132.3; 122.1; 95.0; 91.0; 34.7; 33.7; 31.6. IR (KBr) $\tilde{v}$ (cm^{-1}) 3042 (CH). FAB MS: m/z: 503 [M$^+$ –BF$_4^-$]. Found: C, 48.01; H, 4.35. Calc. for C$_{24}$H$_{26}$B$_2$F$_8$Ru·0.5H$_2$O (598.1): C, 48.19; H, 4.55.

(η^6-Benzene)(η^6-[3$_3$](1,3,5)cyclophane)ruthenium(II) bis(tetrafluoroborate) **14**: Yield 183 mg (79%), faintly greenish yellow crystals (CH$_3$CN–Et$_2$O). ^{1}H-NMR (400 MHz, CD$_3$CN): $\delta = 2.30$–2.84 (m, 18H, –CH$_2$CH$_2$CH$_2$–); 6.43 (s, 3H, H$_b$); 6.45 (s, 6H, H$_a$); 6.91 (s, 3H, H$_c$). ^{13}C-NMR (68 MHz, CD$_3$CN): $\delta =$ 144.3; 132.7; 117.6; 94.8; 90.3; 35.1; 33.8; 30.7. IR (KBr) $\tilde{v}$ (cm^{-1}) 3088 (CH). FAB MS: m/z: 543 [M$^+$ –BF$_4^-$]. Found: C, 51.69; H, 4.79. Calc. for C$_{27}$H$_{30}$B$_2$F$_8$Ru (629.2): C, 51.54; H, 4.81.

(η^6 - Benzene)(η^6 - [3$_4$](1,2,3,5)cyclophane)ruthenium-(II) bis(tetrafluoroborate) **15**: Yield 151 mg (71%), faintly greenish yellow crystals (CH$_3$CN–Et$_2$O). ^{1}H-NMR (400 MHz, CD$_3$CN): $\delta = 2.2$–3.5 (m, 24H, –CH$_2$CH$_2$CH$_2$–); 6.36 (s, 4H, H$_a$); 6.42 (s, 2H, H$_b$); 6.95 (s, 3H, H$_c$). ^{13}C-NMR (100 MHz, CD$_3$CN): $\delta = 143.3$; 142.4; 139.3; 133.7; 120.1; 114.1; 109.0; 94.9; 89.6; 34.7; 33.2; 31.4; 31.2; 31.1; 30.3; 28.3; 26.6; 24.6. IR (KBr) $\tilde{v}$ (cm^{-1}) 3032 (CH). FAB MS: m/z: 583 [M$^+$ –BF$_4^-$]. Found: C, 54.00; H, 5.13. Calc. for C$_{30}$H$_{34}$B$_2$F$_8$Ru (669.3): C, 53.84; H, 5.12.

(η^6-Benzene)(η^6-[3$_4$](1,2,4,5)cyclophane)ruthenium (II) bis(tetrafluoroborate) **16**: Yield 54.8 mg (54%), yellow powder (CH$_3$CN–Et$_2$O). ^{1}H-NMR (270 MHz, CD$_3$CN): $\delta = 2.2$–3.5 (m, 24H, –CH$_2$CH$_2$CH$_2$–); 6.35 (s, 6H, H$_a$); 6.58 (s, 2H, H$_b$); 7.10 (s, 2H, H$_c$). ^{13}C-NMR (68 MHz, CD$_3$CN): $\delta = 140.9$; 134.4; 115.0; 94.8; 90.6; 31.9; 30.0; 29.6. IR (KBr) $\tilde{v}$ (cm^{-1}) 3083 (CH).
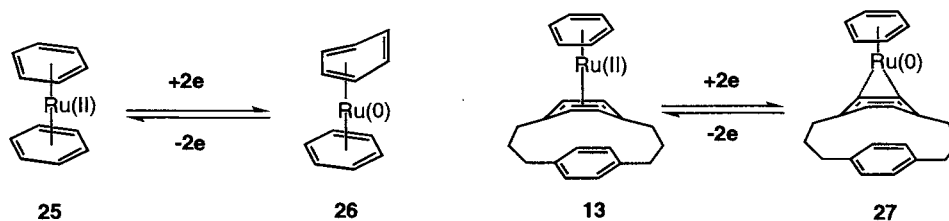
Scheme 6. Reversible redox process, Ru(II) ⇌ Ru(0), of **25** and **13**. The geometrical change is accompanied by the reduction of Ru(II) to Ru(0).

FAB MS: m/z: 583 [$M^+ - BF_4^-$].Found: C, 53.74; H, 5.17. Calc. for $C_{30}H_{34}B_2F_8Ru$ (669.3): C. 53.84; H, 5.12.

4.4. Synthesis of Ru(II) complex, **19**

[(η^6-[3$_2$](l,4)Cyclophane)RuCl$_2$]$_2$ **18**: Yield 247 mg, (76%), red crystals. ^{1}H-NMR (270 MHz, DMSO[D$_6$]): $\delta = 2.1–2.7$ (m, 24H, $-CH_2CH_2CH_2-$); 5.33 (s, 8H, ArH); 6.90 (s, 8H, ArH). FAB MS: m/z: 781 [$M^+ - Cl^-$] Found: C, 53.08; H, 5.06. Calc. for $C_{36}H_{40}C_4Ru_2$ (816.7): C, 52.95; H, 4.94.

Bis(η^6-[3$_2$](1,4)cyclophane)ruthenium(II) bis(tetrafluoroborate) **19**: Yield 322 mg (85%), faintly greenish yellow powder (CH$_3$NO$_2$–Et$_2$O). ^{1}H-NMR (270 MHz, CD$_3$CN): $\delta = 2.1–2.3$ (m, 8H, $-CH_2CH_2CH_2-$); 2.4–2.5 (m, 8H, $-CH_2CH_2CH_2-$); 2.7–2.8 (m, 8H, $-CH_2CH_2CH_2-$); 5.97 (s, 8H, ArH); 6.91 (s, 8H, ArH). ^{13}C-NMR (68 MHz, CD$_3$CN): $\delta = 141.6$; 132.1; 119.3; 90.3; 34.6; 32.9; 31.4. IR (KBr) $\tilde{v}$ (cm^{-1}) 3056 (CH). FAB MS: m/z: 661 [$M^+ - BF_4^-$]. Found: C, 57.35; H, 5.37. Calc. for $C_{36}H_{40}B_2F_8Ru \cdot 0.5H_2O$ (756.4): C, 57.17; H, 5.46.

4.5. Synthesis of Os(II) complexes, **21–24**

(η^6-Benzene)[η^6-[3$_2$](1,4)cyclophane]osmium(II) bis-(hexafluorophosphate) **21**: [(η^6 benzene)Os(II)(CH$_3$- CN)Cl$_2$] **20** (54.6 mg, 0.14 mmol), AgPF$_6$ (80 mg, 0.32 mmol), and acetone (15 ml) were stirred at r.t. for 20 min. The precipitated AgCl was removed by filtration and washed with acetone (ca. 4 ml). The acetone was removed by rotary evaporation, then [3$_2$](1,4)cy-clophane **2** (62.7 mg, 0.26 mmol) and CF$_3$COOH (5 ml) were added and the mixture was refluxed for 2.5 h under N$_2$. The cooled reaction mixture was filtered into an aqueous solution of NH$_4$PF$_6$ to give a white precipitate. The product was collected by filtration, and re-crystallized from acetone–diethyl ether to yield **21** (96.9 mg, 84%) as a white solid. ^{1}H-NMR (270 MHz, CD$_3$CN): $\delta = 2.26–2.91$ (m, 12H, $-CH_2CH_2CH_2-$); 6.60 (s, 4H, H$_b$); 6.68 (s, 6H, H$_a$); 7.07 (s, 4H, H$_c$). ^{13}C-NMR (68 MHz, CD$_3$CN): $\delta = 141.4$; 132.5; 117.5; 88.2; 85.2; 34.6; 33.6; 30.7. IR (KBr) $\tilde{v}$ (cm^{-1}) 3092 (CH). FAB MS: m/z: 651 [$M^+ - PF_6^-$]. Found: C, 36.31; H, 3.36. Calc. for $C_{24}H_{26}F_{12}OsP_2$ (794.6): C, 36.28; H, 3.30.

(η^6-Benzene)(η^6-[3$_3$](1,3,5)cyclophane)osmium(II) bis(hexafluorophosphate) **22**: Yield 74.6 mg (64%), white solid (acetone–Et$_2$O). ^{1}H-NMR (270 MHz, CD$_3$CN): $\delta = 2.31–2.91$ (m, 18H, $-CH_2CH_2CH_2-$); 6.75 (s, 3H, H$_b$); 6.59 (s, 6H, H$_a$); 6.96 (s, 3H, H$_c$). ^{13}C-NMR (l00 MHz, CD$_3$CN): $\delta = 144.1$; 132.8; 112.9; 88.0; 85.4; 35.1; 33.7; 30.0. IR (KBr) $\tilde{v}$ (cm^{-1}) 3092 (CH). FAB MS: m/z: 691 [$M^+ - PF_6^-$]. Found: C,
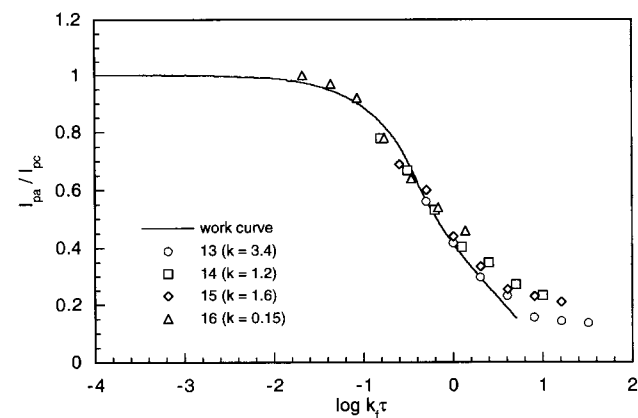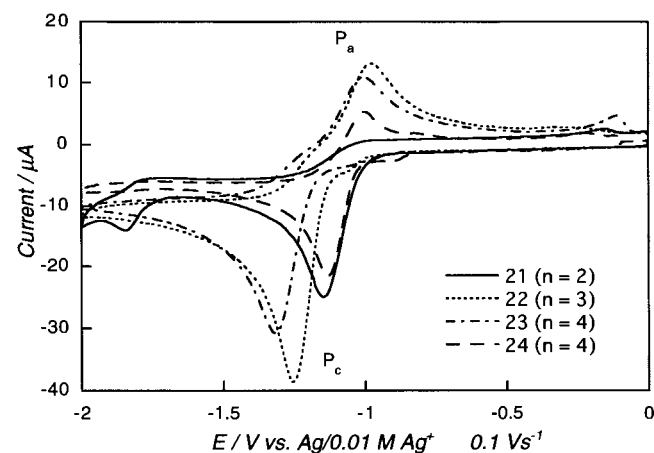

Fig. 5. The theoretical plot of the peak current ratio of P_a to P_c, I_{pa}/I_{pc}, as a function of Log $k_f\tau$, in which τ is the time in seconds between $E_{1/2}$ and the switching potential. The best fitted I_{pa}/I_{pc} curve is obtained at the k_f values of 3.4, 1.2, 1.6 and 0.15 s^{-1} for **13–16**, respectively.
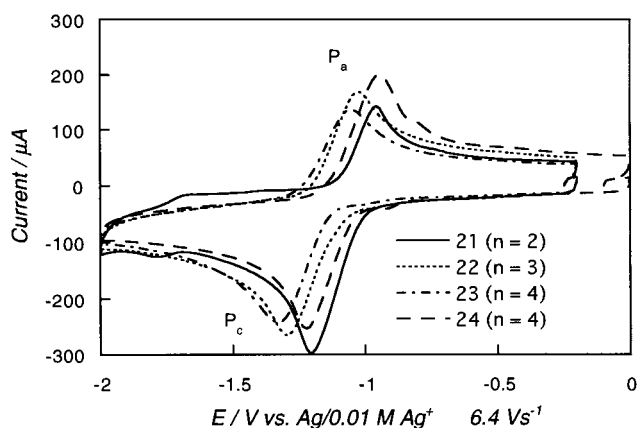

Fig. 6. Cyclic voltammograms of 1 mM **21–24** in CH$_3$CN/0.1 M Bu$_4$NClO$_4$ observed at a GC electrode and potential scan rate of 0.1 V s^{-1}.

Fig. 7. Cyclic voltammograms of 1 mM **21**–**24** in CH_3CN/0.1 M Bu_4NClO_4 observed at a GC electrode and potential scan rate of 6.4 V s^{-1}.

38.91; H. 3.67. Calc. for $C_{27}H_{30}F_{12}OsP_2$ (834.7): C. 38.85; H, 3.62.

(η^6-Benzene)(η^6-[3$_4$](1,2,3,5)cyclophane)osmium(II) bis(hexafluorophosphate) **23**: Yield 70.8 mg (58%), grey solid (acetone–Et$_2$O). ^{1}H-NMR (270 MHz, CD$_3$CN): $\delta = 2.36$–3.27 (m, 24H, –CH$_2$CH$_2$CH$_2$–); 6.52 (s, 4H, H$_a$); 6.76 (s, 2H, H$_b$); 7.02 (s, 3H, H$_c$). ^{13}C-NMR (68 MHz, CD$_3$CN): $\delta = 143.1$; 142.0; 138.7; 133.7; 115.9; 108.4; 104.8; 88.0; 84.8; 34.7; 33.2; 31.4; 31.2; 31.1; 30.3; 28.3; 26.6; 24.6. IR (KBr) $\tilde{v}$ (cm^{-1}) 3098 (CH). FAB MS: m/z: 731 [M$^+$ –PF$_6^-$]. Found: C, 41.17; H, 4.07. Calc. for $C_{30}H_{34}F_{12}OsP_2$ (874.7): C, 41.19; H, 3.92.

(η^6-Benzene)(η^6-[3$_4$](1,2,4,5)cyclophane)osmium(II) bis(hexafluorophosphate) **24**: Yield 69.1 mg (58%), yellow micro crystals (CH$_3$CN–Et$_2$O). ^{1}H-NMR (270 MHz, CD$_3$CN): $\delta = 2.47$–3.14 (m, 24H, –CH$_2$CH$_2$CH$_2$–); 6.52 (s, 6H, H$_a$); 6.95 (s, 2H, H$_b$); 7.20 (s, 2H, H$_c$). ^{13}C-NMR (68 MHz, CD$_3$CN): $\delta = 140.4$; 134.5; 110.7; 87.8; 82.0; 30.9; 29.9; 29.4. IR (KBr) $\tilde{v}$ (cm^{-1}) 3098 (CH). FAB MS: m/z: 731 [M$^+$ –
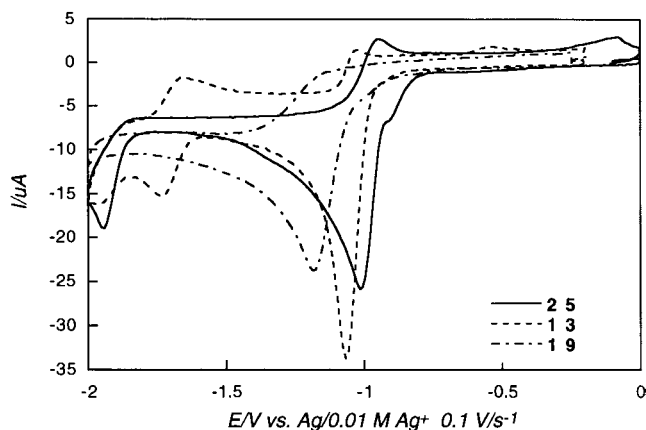
PF$_6^-$]. Found: C, 41.21; H, 3.96. Calc. for $C_{30}H_{34}F_{12}OsP_2$ (874.7): C, 41.19; H, 3.92.

5. Supplementary material available

Part of the electrochemical data of the Ru(II) complexes, Figs. 2, 3, 5 and 8 are available as supplementary material.

References

[1] For a review of transition metal complexes of cyclophanes: J. Schulz, F. Vögtle, in: E. Weber (Ed.), Topics in Current Chemistry vol. 115, Springer-Verlag, Berlin, 1995, p. 41–86.
[2] (a) F.G.N. Cloke, M.L.H. Green, J. Chem. Soc. Dalton Trans. (1981) 1938. (b) F.G.N. Cloke, M.F. Lappert, G.A. Lawless, A.C. Swain, J. Chem. Soc. Chem. Commun. (1987) 1667. (c) J.G. Brennan, F.G.N. Cloke, A.A. Sameh, A. Zalkin, J. Chem. Soc. Chem. Commun. (1987) 1668. (d) D.M. Anderson, F.G.N. Cloke, P.A. Cox, N. Edelstein, J.C. Green, T. Pang, A.A. Sameh, G. Shalimoff, J. Chem. Soc. Chem. Commun. (1989) 53. (e) F.G.N. Cloke, K. Khan, R.N. Perutz, J. Chem. Soc. Chem. Commun. (1991) 1372.
[3] T. Shinmyozu, T. Inazu, T. Yoshino, Chem. Lett. (1977) 1347.
[4] D.J. Cram, R.H. Bauer, J. Am. Chem. Soc. 81 (1959) 5971.
[5] (a) C.J. Brown, J. Chem. Soc. (1953) 3265. (b) P.K. Gantzel, K.N. Trueblood, Acta Crystallogr. 18 (1965) 968.
[6] (a) Y. Sekine, M. Brown, V. Boekelheide, J. Am. Chem. Soc. 101 (1979) 3126. (b) Y. Sekine, V. Boekelheide, J. Am. Chem. Soc. 103 (1981) 1777.
[7] (a) Y. Sakamoto, N. Miyoshi, T. Shinmyozu, Angew. Chem. Int. Ed. Engl. 35 (1996) 549. (b) Y. Sakamoto, N. Miyoshi, M. Hirakida, S. Kusumoto, H. Kawase, J.M. Rudzinski, T. Shinmyozu, J. Am. Chem. Soc. 118 (1996) 12267. (c) Y. Sakamoto, T. Shinmyozu, Recent Research Developments in Pure & Applied Chemistry, Transworld Research Network, 1998 (in press).
[8] The X-ray structural analysis of the CT complex of [3$_6$]cyclophane **1** with tetracyanoquinodimethane (TCNQ) will be reported elsewhere.
[9] The semiempirical MO calculations (PM3) were performed with MOPAC93 program, graphically facilitated by ANCHOR II™ from Fujitsu Limited and Kureha Chemical Industries. (a) J.J.P. Stewart, J. Comput. Chem. 10 (1989) 209. (b) M.J.S. Dewar, E.G. Zoebisch, E.F. Healy, J.J.P. Stewart, J. Am. Chem. Soc. 107 (1985) 3902. (c) J.J.P. Stewart, Fujitsu Limited, Tokyo, Japan, 1993.

Fig. 8. Cyclic voltammograms of 1 mM **13**, **19** and **25** in CH_3CN/0.1 M Bu_4NClO_4 observed at a GC electrode and potential scan rate of 0.1 V s^{-1}.

[10] (a) K. Kurosawa, M. Suenaga, T. Inazu, T. Yoshino, Tetrahedron Lett. 23 (1982) 5335. (b) T. Shinmyozu, Y. Hirai, T. Inazu, J. Org. Chem. 51 (1986) 1551. (c) T. Meno, K. Sako, M. Suenaga, M. Mouri, T. Shinmyozu, T. Inazu, H. Takemura, Can. J. Chem. 68 (1990) 440. (d) K. Sako, T. Meno, H. Takemura, T. Shinmyozu, T. Inazu, Chem. Ber. 123 (1990) 639. (e) T. Shinmyozu, S. Kusumoto, S. Nomura, H. Kawase, T. Inazu, Chem. Ber. 126 (1993) 1815. (f) T. Shinmyozu, M. Hirakida, S. Kusumoto, M. Tomonou, T. Inazu, J.M. Rudzinski, Chem. Lett. (1994) 669. (g) T. Shinmyozu, T. Hirakawa, K. Sako, G. Wen, H. Takemura, J.M. Rudzinski, Liebigs Ann. (1996) 205.

[11] (a) E.D. Laganis, R.G. Finke, V. Boekelheide, Tetrahedron Lett. 21 (1980) 4405. (b) E.D. Laganis, R.H. Voegeli, R.T. Swann, R.G. Finke, H. Hopf, V. Boekelheide, Organometallics 1 (1982) 1415. (c) W.D. Rohrbach, V. Boekelheide, J. Org. Chem. 48 (1983) 3673. (d) R.G. Finke, R.H. Voegeli, E.D. Laganis, V. Boekelheide, Organometallics 2 (1983) 347. (e) R.T. Swann, A.W. Hanson, V. Boekelheide, J. Am. Chem. Soc. 106 (1984) 818. (f) R.T. Swann, A.W. Hanson, V. Boekelheide, J. Am. Chem. Soc. 108 (1986) 3324. (g) R.H. Voegeli, H.C. Kang, R.G. Finke, V. Boekelheide, J. Am. Chem. Soc. 108 (1986) 7010. (h) H.C. Kang, K.-D. Plitzko, V. Boekelheide, J. Organomet. Chem. 321 (1987) 79. (i) K.-D. Plitzko, B. Rapko, B. Gollas, G. Wehrle, T. Weakley, D.T. Pierce, W.E. Geiger Jr., R.C. Haddon, V. Boekelheide, J. Am. Chem. Soc. 112 (1990) 6545. (j) K.-D. Plitzko, G. Wehrle, B. Gollas, B. Rapko, J. Dannheim, V. Boekelheide, J. Am. Chem. Soc. 112 (1990) 6556.

[12] (a) R.T. Swann, V. Boekelheide, J. Organomet. Chem. 231 (1982) 143. (b) E.D. Laganis, R.G. Finke, V. Boekelheide, Proc. Natl. Acad. Sci. USA 78 (1981) 2657. (b) P.F.T. Schirch, V. Boekelheide, J. Am. Chem. Soc. 103 (1981) 6873.

[13] A.R. Koray, J. Organomet. Chem. 212 (1981) 233.

[14] (a) J. Elzinga, M. Rosenblum. Tetrahedron Lett. 23 (1982) 1535. (b) J. Elzinga, M. Rosenblum, Organometallics 2 (1983) 1214.

[15] (a) M.R.J. Elsegood, D.A. Tocher, J. Organomet. Chem. 391 (1990) 239. (b) M.R. Elsegood, D.A. Tocher, Polyhedron 14 (1995) 3147.

[16] (a) J.A. Bandy, M.L.H. Green, D. O'Hare, K. Prout, J. Chem. Soc. Chem. Commun. (1984) 1402. (b) J.A. Bandy, M.L.H. Green, D. O'Hare, K. Prout, J. Chem. Soc. Dalton Trans. (1986) 2477.

[17] (a) T.P. Gill, K.R. Mann, Inorg. Chem. 19 (1980) 3007. (b) T.P. Gill, K.R. Mann, J. Organomet. Chem. 216 (1981) 65. (c) J.L. Schrenk, A.M. McNair, F.B. McCormick, K.R. Mann, Inorg. Chem. 25 (1986) 3501.

[18] A.N. Nesmeyanov, N.A. Vol'kenau, I.N. Bolesova, Dokl. Akad. Nauk. SSSR 149 (1963) 615.

[19] C.C. Lee, B.R. Steele, R.G. Sutherland, J. Organomet. Chem. 186 (1980) 265.

[20] (a) M.A. Bennett, A.K. Smith, J. Chem. Soc. Dalton Trans. (1974) 233. (b) M.A. Bennett, T.W. Matheson, J. Organomet. Chem. 175 (1979) 87.

[21] (a) D.A. Freedman, J.R. Matachek, K.R. Mann, Inorg. Chem. 32 (1993) 1078. (b) D.A. Freedman, D.J. Magneson, K.R. Mann, Inorg. Chem. 34 (1995) 2617.

[22] F.P. Dwyer, J.W. Hogarth, Inorg. Synth. 5 (1957) 206.

[23] T. Miura, T. Horishita, N. Mori, J. Organomet. Chem. 333 (1987) 387 and references therein.

[24] D.T. Pierce, W.E. Geiger, J. Am. Chem. Soc. 111 (1989) 7636.

[25] R.S. Nicholson, I. Shain, Anal. Chem. 36 (1964) 706.

[26] Figure 5 shows the theoretical plot of the I_{pa}/I_{pc} as a function of rate parameter $k_f\tau$, in which τ is the time in seconds between $E_{1/2}$ and the switching potential. The best fitted I_{pa}/I_{pc} curve was obtained with the k_f values of 3.4, 1.2, 1.6 and 0.15 s^{-1} for **13**–**16,** respectively.

[27] A.J. Bard, R.L. Faulkner, Electrochemical Methods, Fundamentals and Applications, Wiley, New York, 1980, pp. 461–465.

[28] W. Sentou, T. Satou, M. Yasutake, C. Lim, Y, Sakamoto, T. Itoh, T. Shinmyozu (accepted for publication).

[29] (a) E.O. Fischer, Ch. Elschenbroich, Chem. Ber. 103 (1970) 162. (b) M. Darensbourg, E.L. Muetterties, J. Am. Chem. Soc. 100 (1978) 7425. (b) E.L. Muetterties, J.R. Bleele., Acc. Chem. Res. 12 (1979) 324. (c) G. Huttner, S. Lange, Acta Crystallogr. B28 (1972) 2049.